

Sulfonated Polybenzimidazoles for High Temperature PEM Fuel Cells

Jordan A. Mader and Brian C. Benicewicz*

Department of Chemistry and Biochemistry and USC NanoCenter, 631 Sumter Street, University of South Carolina, Columbia, South Carolina 29208

Received April 26, 2010; Revised Manuscript Received July 13, 2010

ABSTRACT: High molecular weight, highly PA-doped s-PBI membranes have been developed with robust mechanical properties and excellent proton conductivities ($> 0.1 \text{ S cm}^{-1}$) at elevated temperatures ($> 100^\circ\text{C}$). These membranes show high PA loadings of 30–35 mol PA/PBI, and average tensile stress and strain of 0.804 MPa and 69.64%, respectively. Proton conductivities were dependent on the acid doping level and measured between 0.1 and 0.25 S cm^{-1} at 180°C , a pronounced increase over most phosphoric acid-doped sulfonated PBI membranes to date. Preliminary fuel cell testing with hydrogen fuel and air or oxygen oxidants was performed at temperatures greater than 100°C without external feed gas humidification and show excellent performance (0.62–0.68 V at 0.2 A cm^{-2} and 160°C , hydrogen/air; 0.69–0.76 V at 0.2 A cm^{-2} and 160°C , hydrogen/oxygen). Initial performance stability studies were conducted for $\sim 3000 \text{ h}$ and indicate great promise as high temperature membranes, with a degradation rate of $30 \mu\text{V h}^{-1}$.

Introduction

Over the past decade, polymer electrolyte membrane fuel cells (PEMFCs) have attracted great interest as clean energy devices.¹ These devices have high efficiency and low environmental impact. Much of the research in the past several decades has focused on perfluorosulfonic acid-type membranes such as DuPont's Nafion or similar polymers. While mechanically robust and easily produced, these membranes are limited by their high cost, water-based proton conductivity, and subsequent humidification requirements for medium to high temperature ($> 80^\circ\text{C}$) operation, and susceptibility to catalyst poisoning by impurities such as CO. To overcome these problems, development of low cost alternative membranes for both low and high temperature operation is highly desirable. High temperature operation is particularly attractive because of the potential benefits of faster electrode kinetics, high tolerance to fuel impurities, no humidification requirements, and simplified system design.

Sulfonated aromatic polymers such as polyimides,^{2,3} polysulfones,⁴ polybenzoxazoles,⁵ poly(ether ether ketones),^{6–9} poly(arylene ether)s,^{10–12} and poly(benzobisthiazole)s,¹³ and their copolymers or blends have been widely investigated as alternative membranes. These polymers are significantly cheaper than their fluorinated counterparts, and have begun to show comparable or improved membrane properties, such as water retention, conductivity, and mechanical strength.

A landmark study by Wainright et al.¹⁴ introduced phosphoric acid-doped poly(2,2'-(1,3-phenylene)-5,5'-bibenzimidazole) (*m*-PBI) membranes as promising high temperature PEMFC candidates. Polybenzimidazole is a highly stable aromatic polymer with many commercial uses, including high temperature fibers. The commercially available polymer can be dissolved in organic solvents/inorganic salts (e.g., dimethylacetamide and lithium chloride), cast as a film, dried to remove solvent, washed to remove salts, dried to remove water, and subsequently imbibed in a phosphoric acid (PA) bath to produce PA doped, highly conductive, thermochemically stable membranes.^{14–21} These

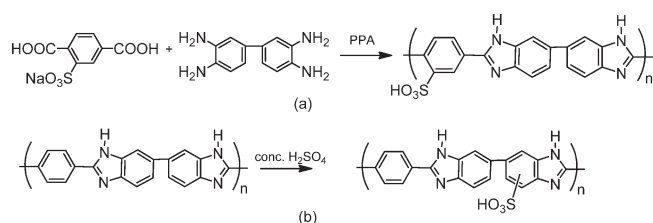
membranes have good ionic conductivities at high temperatures and low humidity ($0.04\text{--}0.08 \text{ S cm}^{-1}$ at 150°C , low doping; 0.13 S cm^{-1} at 160°C , 16 mol PA/PBI), low gas permeability, low electro-osmotic drag coefficient, high CO tolerance, and have exhibited excellent fuel cell performance ($\sim 0.6 \text{ V}$ at 0.20 A cm^{-2} , humidified H_2/O_2 ; $\sim 0.5 \text{ V}$ at 0.2 A cm^{-2} , humidified H_2/Air). A large body of the work on polybenzimidazole derivatives and copolymers/blends/fillers as high temperature fuel cell membranes was recently reviewed.²² Some of the perceived problems with PBI include low molecular weight (inherent viscosities (IVs) of $0.5\text{--}0.8 \text{ dL g}^{-1}$), low phosphoric acid loading (typically 6–10 mol of phosphoric acid per mole polymer repeat unit [moles PA/PBI]), phosphoric acid retention during operation, and membrane durability. The vast majority of PBI research has been done on the commercially available *meta*-PBI or AB-PBI structures.

Recently, a new method to produce highly stable, high molecular weight, robust PBI films has been developed, termed “the PPA process.” This process uses polyphosphoric acid (PPA) as the polycondensation agent, polymerization solvent, and casting solvent. PBIs have been produced from 3,3',4,4'-tetraaminobiphenyl and various dicarboxylic acids.^{23–28} After polymerization, PBI solutions are cast directly from PPA, a hygroscopic material, which then absorbs water from the atmosphere and is hydrolyzed to phosphoric acid (PA) *in situ*. PPA is a good solvent for many PBIs, whereas PA is not. Under the appropriate hydrolysis conditions, a solution to gel (sol–gel) transition occurred, providing a robust PA-doped polymer gel film with excellent physicochemical properties that are not observed from conventional membrane preparation procedures, such as high PA doping levels, extremely robust mechanical properties, excellent conductivities, and excellent long-term stabilities even at high temperatures.

In efforts to capitalize on the early successes of PBI and combine the benefits of high and low temperature membranes, a number of sulfonated derivatives or sulfonated blends with *meta*-PBI have been synthesized.^{13,29–48} Three common approaches are typically employed for functionalizing PBI: (1) direct sulfonation of the backbone,^{29,47,49} (2) chemical grafting of functionalized monomers,^{31,35} or (3) polycondensation of a

*To whom correspondence should be addressed. E-mail: benice@sc.edu. Phone: 803-777-0778. Fax: 803-777-8100.

Scheme 1. Synthetic Scheme of (a) Direct Polymerization of s-PBI from a Sulfonated Diacid and Tetraamine and (b) Post-Sulfonation of *p*-PBI to Produce s-PBI



sulfonated aromatic diacid with an aromatic tetraamine.^{30,50} The last method provides advantages over the first two, such as limitation of side reactions and control over the degree of sulfonation. Previously published work has focused on modification of the *m*-PBI backbone structure.

The sulfonated PBIs (s-PBIs) have typically been proposed as Nafion alternatives and most characterization has been done with water as an electrolyte,^{29–31,34,39,40,43–48} but a small amount of investigation into PA-doped s-PBIs has been performed.^{30,33,38,41,44,46,47} Structures that have been studied include grafting of aryl- or alkyl-sulfonates to the imidazole moiety, postsulfonation onto the biphenyl or diacid phenyl ring, copolymers of sulfonated PBI-type polymers with other sulfonated polymers, postsulfonation of PBI-type polymers with ether linkages incorporated into the backbone, and PBIs made with a sulfonated tetraamine. Initial results show these polymers to be promising low or high temperature membranes, depending on the dopant. The membranes produced are typically high molecular weight, mechanically robust, ionically conductive, and thermally stable at fuel cell operating temperatures, but properties appear to be highly process dependent.^{32,33} Although there has been much characterization of membrane properties, there have been few reports of fuel cell performance published to date.

The work in this paper focuses on the development and characterization of a sulfonated PBI (s-PBI) gel membrane. The PPA process has been shown to produce membranes with improved properties, such as high acid doping levels, high conductivity at high temperature, excellent mechanical properties, and robust fuel cell performance. Phosphoric acid doping (and subsequent polymer and fuel cell characterization) of sulfonated PBIs is relatively unexplored in the literature, and it is of great interest to determine if an additional and stronger acid moiety in the polymer structure will affect the fundamental properties of proton conductivity and fuel cell performance. We report on the synthesis and characterization of a PA-doped sulfonated PBI membrane with high conductivity in low humidity environments, high acid loadings, and robust mechanical properties. Phosphoric acid-doped s-PBI fuel cell performance and long-term testing are reported for the first time and the results demonstrate the excellent thermal and electrochemical stability of the membranes at high temperatures.

Experimental Section

Materials. 2-Sulfoterephthalic acid, monosodium salt (s-TPA, 98%) was purchased from TCI and dried under vacuum prior to use. Terephthalic acid was purchased from Amoco (TPA, 99+%) and used as received. 3,3',4,4'-Tetraaminobiphenyl (TAB, polymer grade) was donated by Celanese Ventures, GmbH and used as received. Polyphosphoric acid (PPA, 115%) was used as supplied from Aldrich Chemical Co. and FMC Corporation. PEEK fleece was obtained from SAATIGroup with a weight of 20 g m⁻², an open area of 79 μm, free surface of 51%, and thickness of 53 μm.

Polymer Synthesis. The PPA process s-PBI homopolymers were synthesized using the following general procedure (Scheme 1a): the

monosodium salt of 2-sulfoterephthalic acid (4.023 g, 15 mmol) and TAB (3.214, 15 mmol) were added to a 100 mL three neck resin reaction flask in a nitrogen atmosphere glovebox, followed by the addition of 107 g of polyphosphoric acid. Monomer concentration at the beginning of the reaction was 4.36 wt % and yielded a 3.5 wt % final polymer concentration. The mixture was stirred by an overhead mechanical stirrer under a slow nitrogen purge. The reaction temperature was controlled by a programmable temperature controller with ramp and soak capabilities. The typical final polymerization temperature was 190 °C for 10–15 h, followed by 4 h at 220 °C to reduce solution viscosity for casting. As the reaction proceeded, the mixture became brown then green and increased in viscosity.

Additionally, postsulfonation of *p*-PBI membranes was pursued for comparison of membrane properties when initial polymer molecular weights were higher. The initial *p*-PBI was synthesized by adding 5.3568 g (25 mmol) TAB and 4.1533 g (25 mmol) of terephthalic acid (TPA) to a 300 mL three neck resin kettle in a nitrogen atmosphere glovebox, followed by the addition of 298.89 g of PPA. The polymerization was performed in a similar method to the s-PBI homopolymer, with a final polymerization temperature of 195 °C for 13 h, before ramping to 220 °C for 1 h to reduce solution viscosity. The polymer was precipitated in water and allowed to hydrolyze for 24 h before being pulverized and neutralized with ammonium hydroxide. The reddish-brown polymer powder was dried under vacuum at 110 °C overnight to remove water before beginning postsulfonation. Following those procedures typical in the literature,⁵¹ 1.0493 g of *p*-PBI was placed in a 400 mL beaker with 250 mL of concentrated sulfuric acid (98%) with stirring. After approximately two hours, the solution was a uniform blue-green color and all polymer had dissolved. A 5 mL aliquot was removed at various time intervals (20, 24, 27, 46, 53, and 92 h) and quenched in ice water. Once quenched, the polymer was washed with ice water until a neutral pH was reached. The polymer was then dried at 110 °C under vacuum overnight before further characterization. It is important to note that using this method, sulfonation is not likely to be selective^{29,47} as indicated in Scheme 1b.

Film Formation. Polymer films were prepared by casting the hot (220 °C) polymer solution onto clean glass substrates using a doctor blade with varying gate thicknesses. Typical casting thicknesses were either 15 or 20 mils (0.381 mm or 0.508 mm). The films were placed in a controlled humidity environment (55 ± 5% RH) at room temperature and allowed to absorb moisture for 24 h to hydrolyze polyphosphoric acid to phosphoric acid. A sol–gel transition was observed during the hydrolysis process which produced a phosphoric acid imbibed gel film.

Characterization Techniques. An aliquot of polymer solution was isolated by precipitation in water as a red-brown solid. This mass was pulverized, stirred with ammonium hydroxide, rinsed to neutrality with distilled water, and dried for 24 h under vacuum at 120 °C to obtain a neutral s-PBI powder for further characterization. Inherent viscosities (IV's) of the polymer samples were then measured at a polymer concentration of 0.2 g dL⁻¹ in concentrated sulfuric acid (96%) at 30 °C, using a Cannon Ubbelohde viscometer. The IV's for the resulting polymers ranged from 0.985 to 1.92 dL g⁻¹ for s-PBI homopolymers. The membrane acid-doping levels were determined by titration of a sample of membrane with standardized sodium hydroxide solution (0.1 N) using a Metrohm 716 DMS Titrino autotitrator. The samples were then rinsed with water and dried in a vacuum oven at 110 °C for 12 h to obtain the dry weight of polymer. The acid-doping level, *X*, expressed as moles of phosphoric acid per mole of PBI repeat unit (*X* mol PA/PBI) were calculated from the equation

$$\text{acid doping level } X = \frac{V_{\text{NaOH}} C_{\text{NaOH}}}{W_{\text{dry}} M_w}$$

where V_{NaOH} and C_{NaOH} are the volume and the molar concentration of the sodium hydroxide titer, W_{dry} is the dry polymer

Table 1. Doped s-PBI Film Properties

batch	monomer conc. (wt %)	polymer conc. (wt %)	IV (dL g ⁻¹)	modulus (MPa)	tensile stress at break (MPa)
1	3.10	2.48	1.08	too weak	too weak
2	3.71	2.97	1.03	2.080	0.270
3	4.35	3.48	1.20	3.188	0.563
4	5.02	4.03	1.31	4.123	0.872
5	5.56	4.48	1.28	5.129	1.193
6	6.18	4.97	1.12	8.604	1.270
7	6.78	5.46	1.19	10.266	1.446
8	7.39	5.96	1.19	15.134	2.246
9 ^a	3.61	3.14	1.71	2.240	0.727
10 ^a	3.54	3.13	1.67	2.415	0.703

^a Batches 9 and 10 were performed after polymerization optimization and were used for fuel cell testing.

weight, and M_w is the molecular weight of the polymer repeat unit. The membrane mechanical properties were tested utilizing an Instron 5846 system with a 100 N load cell and crosshead speed of 10 mm min⁻¹. Dumbbell-shaped specimens were cut following the ASTM standard D683 (Type V specimens). The mechanical properties of all film samples were measured at room temperature in air.

Ionic conductivities were measured using four-probe AC impedance spectroscopy. A Zahner IM6e spectrometer with a frequency range from 1 Hz to 100 kHz was used. A rectangular sample of membrane (3.5 cm × 7.0 cm) was placed in a glass cell with four platinum wire current collectors. Two outer electrodes set 6.0 cm apart on opposite sides of the cell supplied current, while the two inner electrodes 2.0 cm apart on opposite sides of the membrane measured the voltage drop. The cell was placed in a programmable oven to study the temperature dependence of the proton conductivity. Two conductivity runs in air were performed. In the first run, the temperature was increased to 180 °C in 20 degree intervals to remove water, with subsequent cooling under vacuum before performing a second run. The temperature during the second run was increased to 180 °C in 20 degree intervals, and held at 180 °C for 5 h. Before measurement at each temperature set point, the samples were held for at least 15 min for thermal equilibration. For the measurement of conductivity at constant temperature (Figure 3b), the membrane sample was held at 180 °C following the second heating run and proton conductivity was recorded continuously with time during the remaining portion of the experiment. A two-component model with an ohmic resistance in parallel with a capacitor was used to fit the experimental curve of the membrane resistance across the frequency range. The conductivities at different temperatures were calculated from the membrane resistance obtained from the ohmic resistance of the model simulation. Proton conductivity was then calculated from the following equation:

$$\sigma = D/(TWR)$$

where D is the distance between the two inner electrodes, T and W are the membrane thickness and width, respectively, and R is the measured resistance value.

Thermogravimetric analysis (TGA) was performed on a TA Instruments Q5000 IR TGA under a N₂ purge rate of 25 mL min⁻¹ at a heating rate of 10 °C min⁻¹. Attenuated total reflectance (ATR) infrared spectra were recorded using a Perkin-Elmer Spectrum 100 FT-IR with diamond/ZnSe triple reflection crystal.

To investigate alternative applications, other liquids were tested as dopants in the s-PBI system. To dope the membrane with sulfuric acid, the PA-doped s-PBI film from the PPA process was placed in a 30 or 50 wt % sulfuric acid bath and stirred. Films were placed in both heated (~90 °C) and non-heated (room temperature) baths. Films were allowed to equilibrate for at least three days before a small portion was removed for titration and conductivity measurements. Conductivity measurements were performed in the same way as previously described, but the final maximum temperature was changed to

Table 2. Film Formation Results: s-PBI from the PPA Process

batch	casting (wt %)	time at 190 °C	IV (dL g ⁻¹)	film
11	3.48	3	0.89	precipitation
12	3.61	6	0.95	cracked film, mostly precipitated
13	3.54	8	0.99	weak, opaque film, tore when handled
14	3.54	10	1.18	strong film
15	3.99	20	1.19	strong film

100 °C for both runs. Initial conductivity attempts up to 180 °C resulted in a blackened, brittle membrane and failed conductivity curve data collection.

Membrane Electrode Assembly (MEA) Fabrication and Fuel Cell Testing Conditions. The fuel cell gas diffusion electrodes were acquired from BASF Fuel Cell, Inc. with a Pt loading of 1.0 mg cm⁻². The anode was Pt/C and the cathode contained a Pt alloy. The membrane thicknesses were between 175 and 450 μm with PA loadings of 20–52 mol PA/PBI. The MEA was fabricated by hot-pressing an electrode/membrane/electrode sandwich at 4500 lbs and 140 °C for 30–40 s using a manual Carver press. The MEA with an active area of 45.15 cm² was then assembled into a single fuel cell with graphite flow plates on either side of the MEA. Stainless steel end plates with attached heaters were used to clamp the graphite flow plates. A commercial fuel cell testing station (Fuel Cell Technologies, Inc.) equipped with mass flow controllers was used for all testing. Gases were fed to the anode and cathode at a stoichiometric ratio of 1.2 and 2.0, respectively, without any gas humidification. All performance data were collected under atmospheric pressure. The current–voltage performance was recorded using a HP6050 DC electronic load, interfaced with a computer using LabView Software (National Instruments).

Results and Discussion

Synthesis and Characterization of the PPA Process s-PBI Homopolymer. The synthesis of sulfonated polybenzimidazole polymers was investigated via a polycondensation reaction of 2-sulfoterephthalic acid, monosodium salt, and 3,3',4,4'-tetraaminobiphenyl in polyphosphoric acid (PPA), as shown in Scheme 1a, and is referred to as s-PBI. There have been some previous reports in the literature on the development of sulfonated PBIs, but the vast majority of these polymers *N*-alkyl sulfonate on the imidazole/biphenyl moiety and not directly on the phenyl ring portion of the structure. Typically, these membranes are doped with water to produce low temperature proton conducting membranes.

An intensive investigation into the effects of monomer solids on polymer molecular weight was performed. An optimization series of polymerizations with final polymer concentrations from 2.5 to 6.0 wt % was conducted and the inherent viscosity of each polymer was measured. The results are shown in Table 1. The maximum molecular weight of s-PBI was obtained at a final polymer concentration of

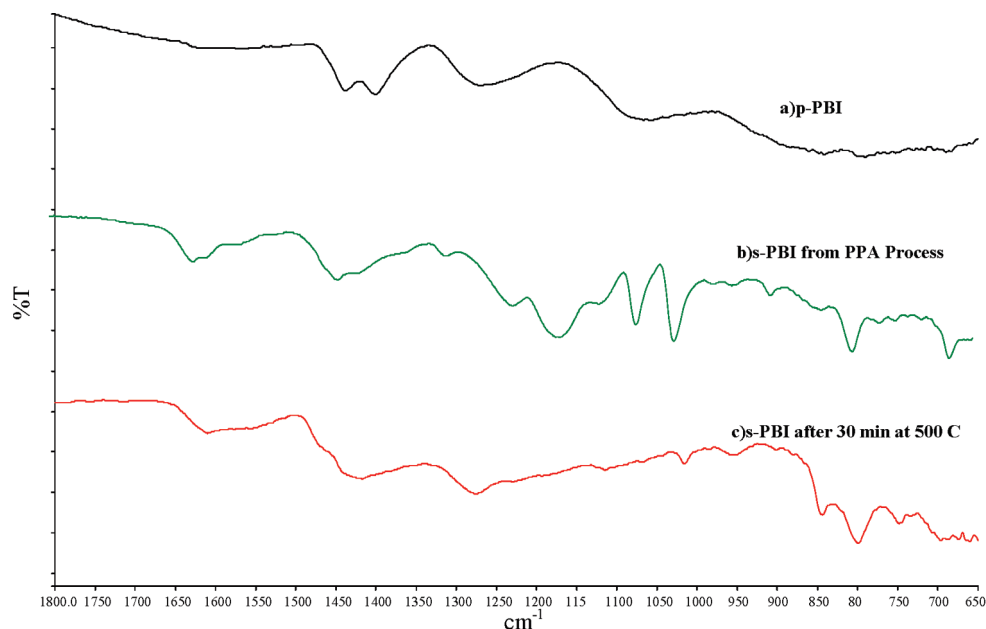


Figure 1. Attenuated total reflectance triple pass infrared spectra of (a) *p*-PBI (black line), (b) s-PBI cast from PPA (green line), and (c) PPA process s-PBI after 30 min of thermal treatment at 500 °C (red line).

4.03 wt %, followed closely by 3.48 and 4.48 wt %. The high IV polymers yielded translucent, red-orange gel films that were mechanically robust. The lower IV films produced from the 2.5 and 3.0 wt % (polymer concentration) polymerizations were opaque orange membranes that broke when handled. The high solids content (5.0–6.0 wt %) polymerizations resulted in mechanically robust gel films with slightly lower IVs. Polymerizations below 2.5 wt % or above 6.0 wt % resulted in polymer precipitation from the cast PPA solution during hydrolysis and inherent viscosities $< 0.95 \text{ dL g}^{-1}$. Further comparison of solids content with other desired fuel cell membrane properties also indicated that the 3.5–4.0 wt % solids membranes provided the best balance of properties and subsequent polymerizations were conducted within these guidelines.

To determine the effects of polymerization time on IV and film formation, a number of polymerizations with polymer solids content of 3.5 wt % were performed. As seen in Table 2, polymerization times of less than 8 h at 190 °C resulted in very weak opaque films or polymer precipitation from solution and IVs less than 1.0 dL g^{-1} . During synthesis, the final polymerization temperature needed to be maintained for at least 8 h to produce a robust gel film, but times greater than 10 h show no additional improvements. It was concluded from these data that polymers with IVs $< 1.0 \text{ dL g}^{-1}$ would not form a gel film, regardless of solids content.

Characterization of s-PBI Films. The polymers were characterized by infrared spectroscopy and thermogravimetric analysis. Triple pass attenuated total reflectance infrared spectroscopy was used to confirm the presence of the sulfonic acid moiety in the polymer structure for PPA Process films. Figure 1 shows the ATR-IR spectra of *p*-PBI and s-PBIs. Three regions of evidence for the presence of the sulfonic acid groups were seen and are consistent with the literature.^{33,35,43} The medium band at 800 cm^{-1} corresponds to the symmetric S–O stretch, whereas the new bands at 1022 and 1070 cm^{-1} arise from the S=O symmetric stretches. The strong bands at 1164 and 1225 cm^{-1} are due to asymmetric stretching of S=O. The band at 1622 cm^{-1} is characteristic of the C=C/C=N stretching vibrations in the imidazole. The absence of a strong band in the 1650 – 1780 cm^{-1} region indicates complete closure of the imidazole ring.

Thermogravimetric scans were performed to determine the stability of the s-PBI polymers at fuel cell operating temperatures (Figure 2). The sulfonic acid group begins decomposition at ~ 425 °C, consistent with the literature^{29,30,34,35,39,43,45–48} and is higher than that of other sulfonated aromatic polymers where significant weight losses are observed above 260 °C.^{40,46} The small weight losses (5–10%) before onset of sulfonic acid decomposition were seen even with drying the sample before testing, and are attributed to water absorbed from the atmosphere during sample transfer due to the hygroscopic nature of PBI, and were also seen in the *p*-PBI trace. The decomposition begins well above fuel cell operating temperatures (> 200 °C), and the homopolymers show excellent thermal stability over this region. In comparison to the *p*-PBI trace, the onset of decomposition at 425 °C on all s-PBI polymers tested confirms the presence of the sulfonic acid functionality. The postsulfonated *p*-PBI also shows a large decomposition trace over the 425–525 °C range, confirming incorporation of the sulfonic acid moiety during the sulfonation procedure.

Phosphoric and Sulfuric Acid Content and Proton Conductivity. A key feature of successful fuel cell membranes is high proton conductivity. Operation of fuel cells above 120 °C is possible with acid-doped membranes and eliminates the reliance on water for proton conductivity. The ionic conductivity of s-PBI was extensively studied in anhydrous conditions from room temperature to 180 °C. In many polymers developed via the PPA Process, there is a minimum phosphoric acid content needed for a membrane to conduct protons effectively and operate in a fuel cell. Typically, a correlation between increased phosphoric acid content (up to 25 mol PA/PBI) and higher conductivity was observed for PPA process PBI chemistries,²³ while doping levels above this value typically show only minor improvements in conductivity.

Phosphoric Acid-Doped Films. Figure 3a shows the ionic conductivity for representative examples of each level of phosphoric acid-doping in the typical s-PBI membranes from room temperature to 180 °C. To remove the contribution of water to the conductivity, the data were collected from the second conductivity run in a temperature controlled

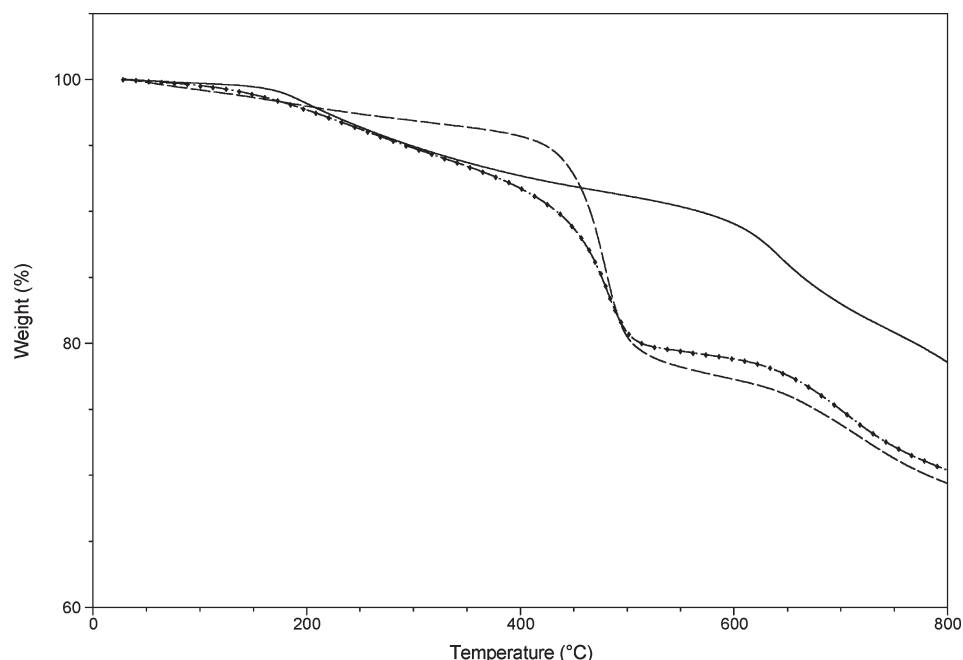


Figure 2. Thermogravimetric analysis of *p*-PBI (solid line), *s*-PBI (dashed line), and postsulfonated *p*-PBI (dash dot line) performed under nitrogen (flow rate of 25 mL min⁻¹) from room temperature to 800 °C.

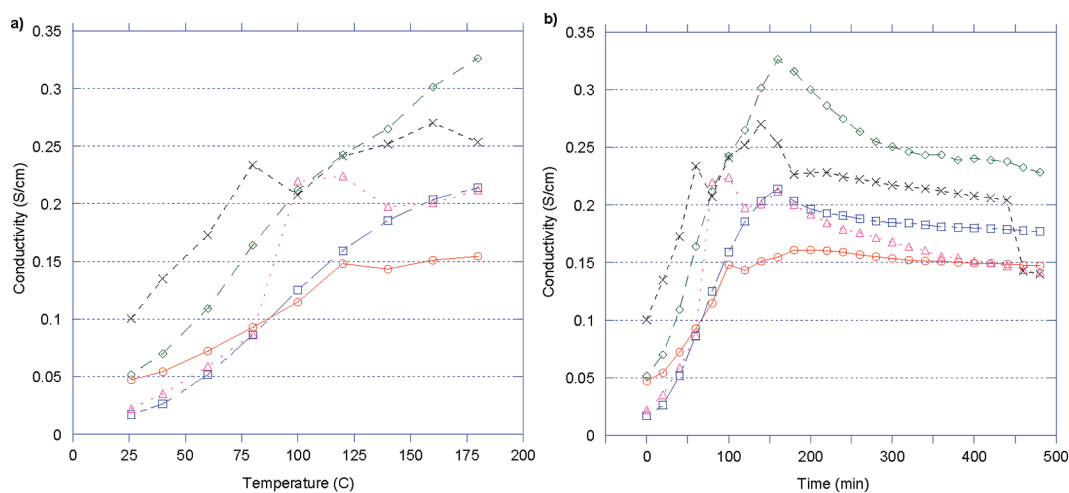


Figure 3. Phosphoric acid-based proton conductivities of *s*-PBI PPA Process membranes from room temperature to 180 °C for (a) short-term and (b) long-term testing (held at 180 °C). Red circles: 28 mol PA/PBI; blue squares: 30 mol PA/PBI; green diamonds: 39 mol PA/PBI; black crosses: 44 mol PA/PBI; pink triangles: 53 mol PA/PBI.

oven with no humidity control. However, due to the hygroscopic nature of both PBI and sulfonated polymers, there was a minor reabsorption of water at lower temperatures, as seen by the small fluctuation in conductivity (80–100 °C) on some of the samples.

Membranes with doping levels of 28–53 mol PA/PBI were tested. All membranes showed excellent conductivities ($> 0.1 \text{ S cm}^{-1}$) at elevated temperatures. Conductivity was affected by phosphoric acid doping level. As the phosphoric acid doping level increased to ~ 40 mol PA/PBI, the ionic conductivity at 180 °C increased, as seen by the 0.161, 0.213, and 0.326 S cm^{-1} values for 28, 30, and 39 mol PA/PBI doping levels, respectively. Doping levels greater than 39 mol PA/PBI did not show any further increase in conductivity. The lower conductivities above 39 mol PA/PBI may be due to limitations of the membranes to hold such large quantities of PA and still maintain mechanical and compositional integrity during testing.

Figure 3b shows the extended conductivity of the *s*-PBI membranes over time. After the initial second conductivity run, the membrane was held at 180 °C while continuously monitoring the proton conductivity. The decrease in conductivity over time is attributed to the removal of additional water by self-condensation of the phosphoric acid to form pyrophosphoric acid ($\text{H}_4\text{P}_2\text{O}_7$).

The conductivity values for sulfonated PBIs in the literature are tabulated in Table 3 and are compared to the *s*-PBI polymers from this work. In comparison to the literature values, even taking structural differences into account, the PA-doped *s*-PBI produced in this work shows significantly higher proton conductivity than nearly all *s*-PBIs reported to date while remaining mechanically robust at higher temperatures and doping levels. This indicates there is a strong dependence of polymerization process on both doping level and conductivity, and is reiterated by Bai and Ho in their work.³³

Table 3. Conductivity Values for Sulfonated Polybenzimidazoles and Copolymers

type of polymer	temp. (°C)	relative humidity (%)	conductivity (S cm ⁻¹)	notes	ref
sulfonated aryl groups on <i>m</i> -PBI	40	100	10^{-4} – 10^{-2} ^b	0.001–1 mol PA dm ⁻³	35
benzylsulfonated <i>m</i> -PBI	NR ^a	NR	3×10^{-3} – 2×10^{-2} ^b	doping level dependent	38
sulfopropyl <i>m</i> -PBI	140	NR	10^{-3} ^c	73.1 mol % sulfonation	40
propyl/butyl sulfonic acid side chain	130	100%	10^{-3} ^c	H ₂ /O ₂ (total <i>P</i> = 3 bar)	31
postsulfonated <i>m</i> -PBI	160	100	7.5×10^{-5} ^c		47
copolymer of sulfonated <i>m</i> -PBI with <i>m</i> -PBI	r.t.	NR	10^{-6} – 10^{-4} ^b	2–3 mol PA/PBI	30
postsulfonated <i>m</i> -PBI with thermal treatment	20	100	2.3 – 7.2×10^{-6} ^c	thermal treatment time dependent	29
4-bromomethyl benzene sulfonate grafted side chain	r.t.	In water	4.69×10^{-4} ^c		44
s-PBI type copolymer	65	85	2.63×10^{-2} ^c	30% s-PBI type	34
s-PBI type copolymer	65	85	8.13×10^{-2} ^c	70% s-PBI type	34
s-PBI type polymer	65	85	9×10^{-2} ^c	homopolymer	34
s-PBI-O (ether link)	120	In water	1.5×10^{-1} ^c	54% degree of sulfonation	48
PBI with sulfonated tetraamine	r.t.	100	8.2×10^{-7} – 3.6×10^{-4} ^c	composition dependent	39
sPBI-OO (two ether links)	120	100	$\sim 8 \times 10^{-2}$ ^c	degree of sulfonation dependent	43
sulfonated <i>m</i> -PBI/ <i>m</i> -PBI-O copolymer	140	50	$\sim 1.9 \times 10^{-1}$ ^b	cast from PPA, 7.7 mol PA/PBI	32, 33
sulfonated <i>m</i> -PBI/ <i>m</i> -PBI-O copolymer	160	30	$\sim 1.8 \times 10^{-1}$ ^b	cast from PPA, 7.7 mol PA/PBI	32, 33
sulfonated <i>m</i> -PBI/ <i>m</i> -PBI-O copolymer	120	50	$\sim 1.9 \times 10^{-2}$ ^b	cast from DMSO, 5.6 mol PA/PBI	32, 33
sulfonated <i>m</i> -PBI	120	100	2.17×10^{-4}	undoped	33
s-PBI, this work	180		1×10^{-1} – 3.26×10^{-1} ^b	28–53 mol PA/PBI	

^aNR: not reported in the reference. ^bPhosphoric acid-doped membrane. ^cWater-doped membrane.

Typical doping levels reported in the literature for *m*-PBI prepared via the conventional organic solvent route are between 6 and 10 mol PA/PBI,^{14,15,17–21} although some films with higher doping levels and poor mechanical properties have been achieved.⁵² Average doping levels for s-PBI membranes developed in this work are between 30 and 35 mol PA/PBI, although some membranes retain 40–50 mol PA/PBI. These values are significantly higher than those reported in the literature to date for conventionally prepared PBI membranes. Sulfonated PBIs that have been previously produced and doped with phosphoric acid typically contain 2–8 mol PA/PBI^{30,33,35,38,41,46,47} which is considerably lower than the membranes produced via the PPA Process. The s-PBI membranes retain excellent mechanical properties, even at high doping levels.

However, s-PBI membranes with doping levels as low as 20 mol PA/PBI exhibit conductivities of ≥ 0.1 S cm⁻¹ at 180 °C. The previously reported values for phosphoric acid-doped *m*-PBI are 2.5×10^{-3} S cm⁻¹ at 130 °C for PA doping level of 380 mol % to 4.6×10^{-2} S cm⁻¹ at 165 °C for a membrane with 450 mol % acid content^{53,54} while those for the conventionally produced sulfonated PBIs are typically considerably lower.

Sulfuric Acid-Doped Films. PBI is known to be thermally stable in harsh environments even at high temperatures. Additionally, the TGA data in Figure 2 shows the sulfonic acid groups to be thermally stable at fuel cell operating temperatures. In this work, a sulfonated PBI membrane doped with sulfuric acid was investigated for the first time as a proton conducting membrane.

SA-doped s-PBI films were produced as described in the Experimental Section. The titration results (Table 4) show an increase in polymer weight of the membrane compared to the original PA-doped s-PBI, which indicates that additional sulfonation of the membrane may be occurring. Higher temperatures typically increased the rate and level of sulfonation, which was seen by the increase in polymer weight between the heated and room temperature baths of the same concentration, even when the acid doping levels were higher for the room temperature baths. The high acid loading levels (> 25 mol SA/PBI) are comparable to the PA-doped film and thus were subsequently evaluated as proton conductive membranes.

The ionic conductivities of SA-doped films were tested as previously described and are shown in Figure 4. The ionic

Table 4. Acid Content of Sulfuric and Phosphoric Acid-Doped s-PBI

film	polymer contents (g)	acid loading (mol acid/PBI)
PA-doped s-PBI	0.0413	39.84
30 wt % SA room temp bath	0.0516	25.47
30 wt % SA heated bath	0.0553	30.36
50 wt % SA room temp bath	0.0583	50.49
50 wt % SA heated bath	0.0587	31.48

conductivities of these membranes are extremely high (≥ 0.1 S cm⁻¹ at room temperature), even at elevated temperatures (0.24–0.54 S cm⁻¹ at 80–100 °C). The conductivity decreases with time at 100 °C (0.13–0.35 S cm⁻¹), but remains well above the values for water-doped sulfonated membranes reported in the literature. The 30 wt % room temperature bath yielded the membrane with the highest conductivities at all temperatures and also over time, while the 50 wt % room temperature bath membrane also had excellent conductivities over the temperature range. The heated baths gave membranes with lower initial conductivities and larger decreases in performance over time. This is likely due to the lower initial water content and higher polymer content, as well as the dimensional changes, allowing less void space for incorporation of dopant. Additionally, the changes in chemical structure from reactions in the sulfuric acid bath may cause lower conductivity. However, the excellent conductivities reported in this initial evaluation warrant further testing for new applications using these SA-doped membranes.

Membrane Mechanical Properties. A detailed investigation into the mechanical properties of the PA-doped s-PBI membranes was performed. Due to the corrosive nature of sulfuric acid, the SA-doped membrane mechanical properties were not tested. After hydrolysis, the s-PBI gel membranes contained between 2.5 and 6.0 wt % solids and 97.5–94% phosphoric acid and water. Due to the composition and nature of a gel film, lower mechanical properties compared to the fully dense films cast from organic solvents would be expected. No overall correlations could be seen for this group of membranes, because the mechanical properties arise from the interaction of molecular weight, solids content, and acid doping levels, but properties ranged from 0.270 to 2.24 MPa tensile stress and 23–230% tensile strain at break. For membranes with a solids content of ~ 3.0 – 3.5 wt %, the average tensile stress at break was 0.804 MPa, with

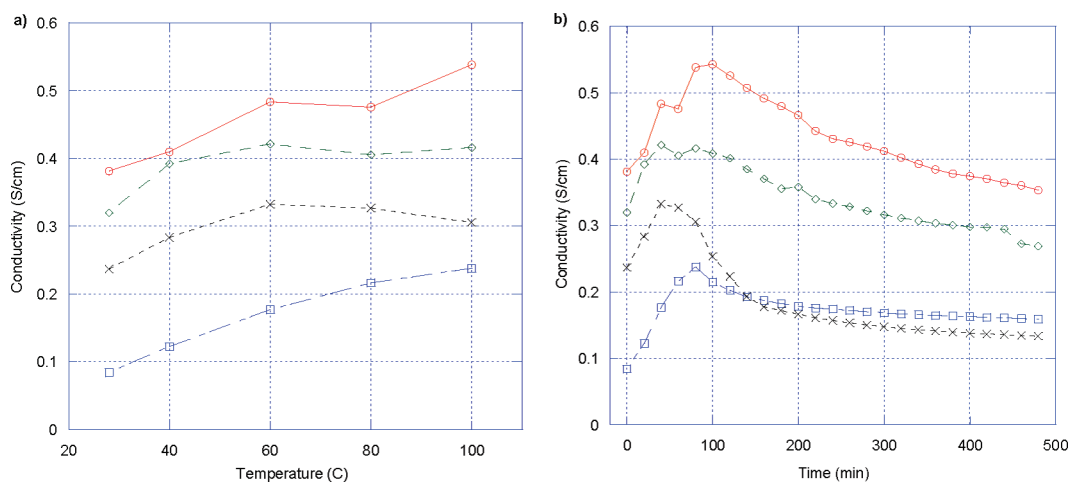


Figure 4. Sulfuric acid-doped s-PBI membranes from room temperature to 100 °C for (a) short-term and (b) long-term testing (held at 100 °C). Red circles: 30 wt % room temperature sulfuric acid bath; blue squares: 30 wt % heated sulfuric acid bath; green diamonds: 50 wt % room temperature sulfuric acid bath; black crosses: 50 wt % heated sulfuric acid bath.

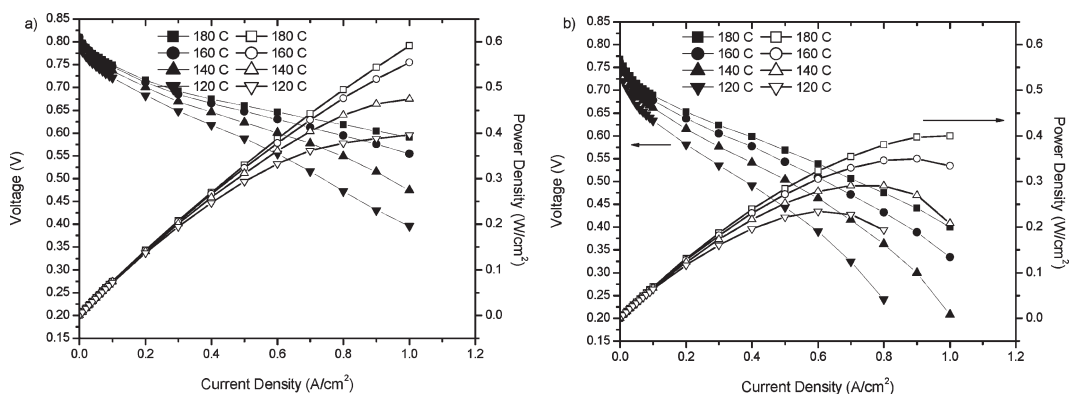


Figure 5. Fuel cell performance of PA-doped s-PBI (3.13 wt % polymer, IV = 1.67 dL g⁻¹, and 28.41 mol PA/PBI): polarization curves (filled symbols) and power density curves (open symbols) with (a) hydrogen and oxygen and (b) hydrogen and air.

Table 5. Summary of s-PBI Fuel Cell Performance

film no.	H ₂ /Air ^a	H ₂ /O ₂ ^a	lifetime loss (mV h ⁻¹)	wt % polymer	IV (dL g ⁻¹)	PA doping (mol PA/PBI)
1	0.6788	0.7559		3.14	1.71	52.33
2	0.6379	0.7114	-0.25	3.13	1.67	28.41
3	0.6347			3.03	1.80	30.07
4	0.6167		-0.014	3.03	1.26	28.29
5	0.6260	0.6930		3.54	1.18	32.72

^a Voltages measured at 160 °C and current density of 0.2 A cm⁻²

an average tensile strain of ~70%. The maximum tensile stress and strain observed were 1.556 MPa and 232%, respectively. There are few reports of acid-doped s-PBI membrane mechanical properties in the literature, but compared to other PPA Process membranes with values of 3–3.5 MPa tensile stress and 400–450% elongation for polymers with IVs of 2–3 dL g⁻¹,²⁴ the values seen for s-PBI are considerably lower. This may be largely influenced by the lower molecular weights of s-PBI polymers (< 2.0 dL g⁻¹) compared to the other chemistries developed through the PPA Process. In general, it was observed that higher solids content in the gel film led to higher tensile strength and lower IV's led to poor mechanical properties. However, the fuel cell performance of many of these membranes confirmed that the mechanical properties of s-PBI are sufficiently high for fuel cell fabrication and operation at high temperatures.

Fuel Cell Performance. Membranes with high IV's (> 1 dL g⁻¹) and high membrane mechanical properties were fabricated into MEAs and tested in fuel cells. Figure 5 shows the

performance characteristics of a typical s-PBI membrane. Table 5 summarizes the fuel cell performance of s-PBI membranes at 160 °C for several membranes with different polymer IVs and membrane PA doping levels.

The highest performance at 0.2 A cm⁻² and 160 °C (0.679 V) was seen from an s-PBI membrane with high IV and the highest acid loading and conductivity of the membranes tested, while the lowest performance (0.6167 V) was seen from the membrane with the lowest acid loading and IV, but not the lowest conductivity. Thus, there appears to be some correlation between phosphoric acid loading and performance, but no direct relationship between conductivity and performance. Further investigation into these relationships is currently being pursued. The performance of the membranes was greatly increased when the oxidant gas was switched to oxygen, as seen by the absence of tailing at higher current densities caused by mass transport limitations. There was a ~67–77 mV improvement in performance across the membranes at 160 °C and 0.2 A cm⁻² when oxygen

was used. The theoretical increase in performance when using oxygen in place of air is ~ 65 mV. The greater than theoretical improvement is likely due to the unoptimized MEA fabrication pressing conditions for these membranes during the course of this work.

Figure 6 shows the first report of long-term performance of an acid doped s-PBI membrane. The performance is significantly improved over the water-doped sulfonated PBI membranes reported to date.³¹ A preliminary long-term test was performed with s-PBI ($IV = 1.67$ dL g⁻¹, PA loading = 28.41 mol PA/PBI, conductivity = 0.161 S cm⁻¹) where the membrane was operated for 400 h at 0.2 A cm⁻² and 160 °C. The operating voltage decreased at the rate of 0.25 mV h⁻¹ over the test period. At 400 h, performance declined slightly and the fuel cell was shut down. A second s-PBI membrane was tested for 1200 h and showed very small performance loss over time (-0.014 mV h⁻¹). These first long-term tests of s-PBI doped with PA demonstrate that these materials are good candidates for high temperature PEMFCs.

To improve the mechanical properties of s-PBI membranes, porous membrane supports were investigated. The viscous solution of s-PBI in PPA was cast on top of a poly(ether ether ketone) (PEEK) fleece mesh. The membrane was hydrolyzed under typical conditions (room temperature, $55 \pm 5\%$ RH) and the normal polymer characterization was performed. It was found that the PEEK fleece did not

adversely affect membrane formation or general characteristics, as seen by $IV = 1.15$ dL g⁻¹, 4.80 wt % solids, 53 mol PA/PBI, and conductivity of 0.208 S cm⁻¹. The hydrogen/air polarization curves over time and long-term performance are shown in Figure 7. The performance of the membrane at 160 °C increased for ~ 420 h, then started a very slow decline for the next 2500 h, at a rate of -0.030 mV h⁻¹, before failing at ~ 2850 h, likely due to membrane creep, as evidenced by examination of the MEA after cell disassembly.

There is little fuel cell performance reported to date for other sulfonated PBIs,^{31,41,47} although some data is available with a water dopant. Staiti et al. reported testing a post-sulfonated PBI in a hydrogen/oxygen (3 bar/5 bar) fuel cell from 80 to 120 °C with humidified gases.⁴⁷ The OCV was 0.9 V, but when a load was applied to the cell, the voltage immediately dropped to zero. Bae et al. developed a propyl-sulfonate-grafted *m*-PBI and tested a humidified hydrogen/oxygen fuel cell at 80 °C and reported a performance of ~ 0.45 V at 0.2 A cm⁻².³¹ Additionally, an MEA with catalyst loading of 0.4 mg cm⁻² Pt catalyst was prepared from the butylsulfonate-grafted *m*-PBI backbone. This membrane, tested under hydrogen/oxygen at 80 °C and ambient total pressure with 100% RH, showed a maximum performance of 0.2 W cm⁻² at 0.7 A cm⁻² (corresponding voltage of 0.29 V) in a water-based system. There are limited acid-doped reports of PA-doped PBI fuel cell performance.^{55–57} Wang et al. tested commercially available (nonsulfonated) *m*-PBI doped in 5 M PA in a humidified H₂/O₂ fuel cell at 150 °C for 200 h at a constant cell voltage of 0.55 V with almost no performance loss and excellent fuel cell characteristics.⁵⁵ Li et al.⁵⁷ reported fuel cell testing for nonhumidified H₂/O₂ (3/3 bar) acid-doped *m*-PBI cells. The maximum performance achieved at 200 °C was 1.0 W cm⁻², but the doping level was not reported. A H₂/O₂ 10 cm² cell with Pt catalyst loading of 0.51 mg cm⁻², and hydrogen flow rate of 30 mL min⁻¹ cm⁻² showed a performance of ~ 0.65 V at 0.2 A cm⁻² at 100 °C. Additionally, stable long-term testing at 0.5 V for 3500 and 5000 h was reported at 120 and 150 °C, respectively. Savinell reported testing PA-doped (nonsulfonated) *m*-PBI (5 mol PA/PBI) with humidified H₂/O₂ and methanol/O₂ at 150 °C, with E-TEK electrodes with a Pt loading of 0.5 mg cm⁻².⁵⁶ These cells reported a maximum power of 0.25 W cm⁻² at 0.700 A cm⁻², which corresponds to a voltage of 0.357 V. Additionally, the cell was operated continuously at 0.2 A cm⁻² for 200 h with no loss of performance. In comparison, the s-PBIs in this work range from 0.411 V– 0.519 V (~ 0.288 – 0.364 W cm⁻²) at 160 °C and 0.7 A cm⁻² with air and 0.486 – 0.690 V (0.340 – 0.483 W cm⁻²)

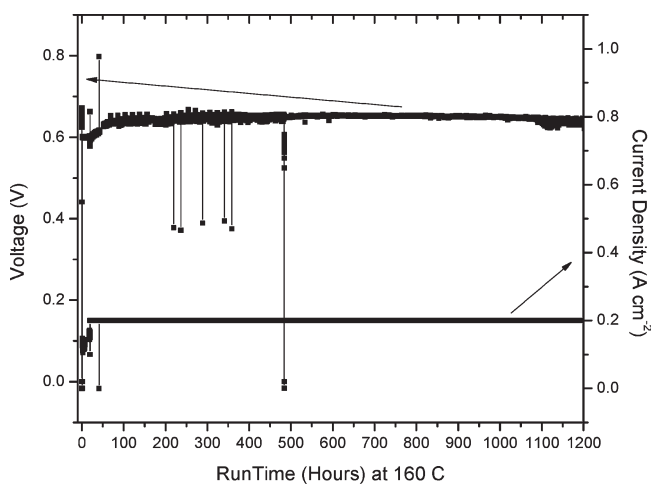


Figure 6. Long-term hydrogen/air fuel cell performance at 160 °C and constant current density of 0.2 A cm⁻² for s-PBI with 3.03 wt % solids, $IV = 1.28$ dL g⁻¹, 28 mol PA/PBI.

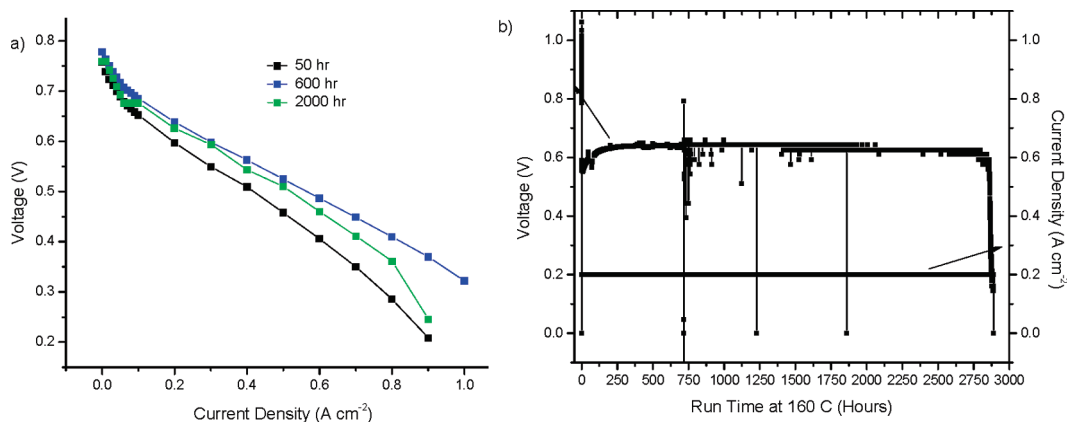


Figure 7. Hydrogen/air fuel cell performance of s-PBI with porous PEEK fleece support (4.80 wt % solids, $IV = 1.15$ dL g⁻¹, 53 mol PA/PBI): (a) polarization curves over time at 160 °C and (b) long-term performance at 160 °C and 0.2 A cm⁻².

with oxygen. This is an increase in performance of ~50–162 mV using air and ~90–230 mV with oxygen over the literature values.

Conclusions

A series of polybenzimidazoles containing sulfonic acid groups on the main chain phenyl ring were synthesized using polyphosphoric acid (PPA) as the reaction and casting solvent. Following an investigation of the synthetic conditions, high molecular weight s-PBI homopolymer was produced as indicated by IV measurements. These polymers were characterized with respect to important fuel cell membrane properties, and it was found that the PPA-cast membranes had high molecular weight, phosphoric acid doping levels, ionic conductivity, and excellent mechanical properties.

Polymer and film properties were highest for those PPA Process membranes with a final membrane solids content of 3.5–4.0 wt % and IV's > 1.0 dL g⁻¹. Phosphoric acid loading levels ranged between 22 and 55 mol PA/PBI, depending on polymer synthesis and casting conditions. Sulfuric acid was studied as an alternative dopant, and highly acid loaded, highly conductive films were produced with excellent thermochemical stabilities up to 100 °C. These films show promise for lower temperature fuel cell or alternative membrane applications.

The thermal stability of the PBI backbone and sulfonic acid functional group at fuel cell operating temperatures and in acidic conditions was shown via TGA. The incorporation of the sulfonic acid group into the postsulfonated *p*-PBI was suggested from the TGA studies and the structure was confirmed by ATR-IR studies. A detailed study on fuel cell performance and long-term durability is reported for the first time and was used to fully evaluate the PA-doped sulfonated PBI membranes. Acid doping level was found to contribute to fuel cell performance; a s-PBI membrane with doping level of 52 mol PA/PBI showed a ~41 mV improvement (160 °C, 0.2 A cm⁻²) over a membrane with a doping level of 28 mol PA/PBI. Hydrogen-air performance was improved over previously reported water-doped sulfonated polybenzimidazole membranes and conventionally produced and doped *m*-PBI membranes. It was found that s-PBI performance increased greatly when oxygen gas was used as the oxidant. The s-PBI membranes showed excellent long-term stability using hydrogen-air with testing conducted for ~2900 h with a degradation rate of -0.030 mV h⁻¹.

In comparison to sulfonated polybenzimidazoles produced previously, and to the conventionally prepared PBI membranes, the PA-doped s-PBI gel membranes produced via the PPA Process show greatly improved properties and fuel cell performance with both oxygen and air as oxidants and no external humidification of feed gases. By supplementing the mechanical properties of the s-PBI membranes with a PEEK fleece, preliminary long-term performance data were obtained for the s-PBI homopolymers that indicates feasibility in fuel cell applications.

Acknowledgment. The authors gratefully acknowledge the financial and technical support of BASF Fuel Cell, Inc. and Dr. G. Calundann.

References and Notes

- Carrette, L.; Friederich, K. A.; Stimming, U. *ChemPhysChem* **2000**, *1*, 162–93.
- Faure, S.; Mercier, R.; Aldebert, P.; Pineri, M.; Sillion, B. French patent 9605707, 1996.
- Watari, T.; Fang, J.; Tanaka, K.; Kita, H.; Okamoto, K.-I.; Hirano, T. *J. Membr. Sci.* **2004**, *230*, 111–120.
- Lufrano, F.; Gatto, I.; Staiti, P.; Antonucci, V.; Passalacqua, E. *Solid State Ionics* **2001**, *145*, 47–51.
- Einsla, B. R.; Harrison, W. L.; Tchatchoua, C.; McGrath, J. E. *Polym. Prepr.* **2004**, *44*, 645–646.
- Gao, Y.; Robertson, G. P.; Guiver, M. D.; Mikhailenko, S. D.; Kaliaguine, S. *Macromolecules* **2004**, *37*, 6748–6754.
- Gil, M.; Ji, X.; Li, X.; Na, H.; Hampsey, J. E.; Lu, Y. *J. Membr. Sci.* **2004**, *234*, 75–81.
- Jin, X.; Bishop, M. T.; Ellis, T. S.; Karasz, F. E. *Br. Polym. J.* **1985**, *17*, 4–10.
- Xing, P.; Robertson, G. P.; Guiver, M. D.; Mikhailenko, S. D.; Kaliaguine, S. *Macromolecules* **2004**, *37*, 7960–7967.
- Hickner, M. A.; Ghassemi, H.; Kim, Y. S.; Einsla, B. R.; McGrath, J. E. *Chem. Rev.* **2004**, *104*, 4587–4612.
- Wang, F.; Hickner, M.; Kima, Y. S.; Zawodzinski, T. A.; McGrath, J. E. *J. Membr. Sci.* **2002**, *197*, 231–242.
- Xiao, G. Y.; Sun, G. M.; Yan, D. Y.; Zhu, P. F.; Tao, P. *Polym. Prepr.* **2002**, *43*, 5335–5339.
- Kim, S.; Cameron, D. A.; Lee, Y.; Reynolds, J. R.; Savage, C. R. *J. Polym. Sci., Part A: Polym. Chem.* **1996**, *34*, 481–492.
- Wainright, J. S.; Wang, J. T.; Weng, D.; Savinell, R. F.; Litt, M. *J. Electrochem. Soc.* **1995**, *142*, L121–L123.
- Bouchet, R.; Siebert, E. *Solid State Ionics* **1999**, *118*, 287–299.
- Cassidy, P. E. In *Thermally stable polymers: synthesis and properties*. Marcel Dekker, Inc.: New York, 1980; Sections 6.10 and 6.18–20.
- Kerres, J.; Ullrich, A.; Meier, F.; Haring, T. *Solid State Ionics* **1999**, *125*, 243–249.
- Kim, H.; Lim, T. *Ind. Eng. Chem.* **2004**, *10*, 1081–1085.
- Li, Q.; He, R.; Gao, J.; Jensen, J. O.; Bjerrum, N. J. *J. Electrochem. Soc.* **2003**, *150*, A1599–A1605.
- Ma, Y. L.; Wainright, J. S.; Litt, M. H.; Savinell, R. F. *J. Electrochem. Soc.* **2004**, *151*, A8–A16.
- Samms, S. R.; Wasmus, S.; Savinell, R. F. *J. Electrochem. Soc.* **1996**, *143*, 1225–1232.
- Mader, J.; Xiao, L.; Schmidt, T.; Benicewicz, B. C. In *Advances in Polymer Science, Special Vol. Fuel Cells*; Scherer, G., Ed.; Springer-Verlag: New York, 2008; Vol. 216, p 63.
- Yu, S.; Benicewicz, B. C. *Macromolecules* **2009**, *42*, 8640–8648.
- Xiao, L.; Zhang, H.; Jana, T.; Scanlon, E.; Chen, R.; Choe, E. W.; Ramanathan, L. S.; Yu, S.; Benicewicz, B. C. *Fuel Cells* **2005**, *5*, 287–295.
- Xiao, L.; Zhang, H.; Jana, T.; Scanlon, E.; Ramanathan, L. S.; Choe, E. W.; Rogers, D.; Apple, T.; Benicewicz, B. C. *Chem. Mater.* **2005**, *17*, 5328–5333.
- Qian, G.; Smith, D. W.; Benicewicz, B. C. *Polymer* **2009**, *50*, 3911–3916.
- Qian, G.; Benicewicz, B. C. *J. Polym. Sci., Part A: Polym. Chem.* **2009**, *47*, 4064–4073.
- Yu, S.; Xiao, L.; Benicewicz, B. C. *Fuel Cells* **2008**, *8*, 165–174.
- Ariza, M. J.; Jones, D. J.; Roziere, J. *Desalination* **2002**, *147*, 183–189.
- Asensio, J. A.; Borros, S.; Gomez-Romero, P. *J. Polym. Sci., Part A: Polym. Chem.* **2002**, *40*, 3703–3710.
- Bae, J. M.; Honma, I.; Murata, M.; Yamamoto, T.; Rikukawa, M.; Ogata, N. *Solid State Ionics* **2002**, *147*, 189–194.
- Bai, H.; Ho, W. S. W. *Ind. Eng. Chem.* **2009**, *48*, 2344–2354.
- Bai, H.; Ho, W. S. W. *J. Taiwan Instit. Chem. Eng.* **2009**, *40*, 260–267.
- Bai, Z.; Price, G. E.; Yoonessi, M.; Juhl, S. B.; Durstock, M. F.; Dang, T. D. *J. Membr. Sci.* **2007**, *305*, 69–76.
- Glipa, X.; El Haddad, M.; Jones, D. J.; Roziere, J. *Solid State Ionics* **1997**, *97*, 323–331.
- Hasiotis, C.; Deimede, V.; Kontoyannis, C. *Electrochim. Acta* **2001**, *46*, 2401–2406.
- Hasiotis, C.; Li, Q.; Deimede, V.; Kallitsis, J. K.; Kontoyannis, C. G.; Bjerrum, N. G. *J. Electrochem. Soc.* **2001**, *148*, A513–A519.
- Jones, D. J.; Roziere, J. *J. Membr. Sci.* **2001**, *185*, 41–58.
- Jouanneau, J.; Mercier, R.; Gonon, L.; Gebel, G. *Macromolecules* **2007**, *40*, 983–990.
- Kawahara, M.; Rikukawa, M.; Sauni, K. *Polym. Adv. Technol.* **2000**, *11*, 544–547.
- Kim, H.-J.; Lee, J. W.; Lim, T.-H.; Nam, S. W.; Hong, S.-A.; Oh, I.-H.; Ham, H. C.; Lee, S.-Y. U.S. Patent 0241627A1, 2008.
- Kosmala, B.; Schauer, J. *Appl. Polym. Sci.* **2002**, *85*, 1118–1127.
- Peron, J.; Ruiz, E.; Jones, D. J.; Roziere, J. *J. Membr. Sci.* **2008**, *314*, 247–256.
- Pu, H.; Liu, Q. *Polym. Int.* **2004**, *53*, 1512–1516.
- Qing, S.; Huang, W.; Yan, D. *Eur. Polym. J.* **2005**, *41*, 1589–1595.
- Rikukawa, M.; Sanui, K. *Prog. Polym. Sci.* **2000**, *25*, 1463–1502.
- Staiti, P.; Lufrano, F.; Arico, A. S.; Passalacqua, E.; Antonucci, V. *J. Membr. Sci.* **2001**, *188*, 71–78.

- (48) Xu, H.; Chen, K.; Guo, X.; Fang, J.; Yin, J. *Polymer* **2007**, *28*, 5556–5564.
- (49) Asensio, J. A.; Borros, S.; Gomez-Romero, P. *Electrochim. Acta* **2004**, *49*, 4461–4466.
- (50) Sakaguchi, Y.; Kitamura, K.; Nakao, J.; Hamamoto, S.; Tachimori, H.; Takase, S. *Polym. Mater. Sci. Eng.* **2001**, *84*, 899–900.
- (51) Yang, B.; Manthiram, A. *Electrochem. Solid-State Lett.* **2003**, *6*, A229–A231.
- (52) Li, Q.; Hjuler, H. A.; Bjerrum, N. J. *J. Appl. Electrochem.* **2001**, *31*, 773–779.
- (53) Savinell, R. F.; Litt, M. H. WO Patent 9737396, 1997.
- (54) Wang, J. T.; Wainright, J.; Yu, H.; Litt, M.; Savinell, R. F. *Proc. Electrochem. Soc.* **1995**, *95*, 202–213.
- (55) Wang, J. T.; Savinell, R. F.; Wainright, J.; Litt, M.; Yu, H. *Electrochim. Acta* **1996**, *41*, 193–197.
- (56) Savinell, R. F.; Yeager, E.; Tryk, D.; Landau, U.; Wainright, J. S.; Weng, D.; Lux, K.; Litt, M.; Rogers, C. J. *Electrochem. Soc.* **1994**, *141*, L46–L48.
- (57) Li, Q.; He, R.; Jensen, J. O.; Bjerrum, N. J. *Fuel Cells* **2004**, *4*, 147–159.